



Our Extremely Quiet and Oil-free Vacuum Pumps of the HiScroll® Series

Your added value

- Low noise, low vibration
- Lowest operating costs through fully automatic pressure regulation
- Safe due to built-in non-return valve and hermetically sealed pump system
- Optimal process adaptation through intelligent interface technology
- Compact design for use in analysis systems/ laboratory equipment

Mapping and imaging of thin films on large surfaces

Peter Petrik^{1*} | Miklos Fried^{1*}

¹Institute of Technical Physics and
Materials Science, Centre for Energy
Research, Konkoly Thege Rd. 29-33, 1121
Budapest, Hungary

Correspondence

Peter Petrik

Email: petrik.peter@ek-cer.hu

Funding information

Thin films covering large surfaces are used in a very wide range of applications from displays through corrosion resistance, decoration, water proofing, smart windows, adhesion performance to solar panels and many more. Scaling up existing thin film measurement techniques requires a high speed and the redesign of the configurations. The aim of this review is to give an overview of recent and past activities in the area, as well as an outlook of future opportunities.

Keywords: Thin film measurement, ellipsometry, reflectometry, optical mapping, nanolayer characterization

1 Introduction

Methods of in-depth thin film characterization [1] based on either depth profiling by sputtering, complex modeling based on nondestructively measured whole-depth data, or preparing cross-sections destructively and time-consuming are all mature to an extent that only requires incremental adaptations and improvements for new tasks such as large-area mapping. In Ref. [2] further methods for the determination of coating thickness are reviewed with in-line and offline capabilities. There are intrinsic features of those methods that make only a few of them capable of collecting the amount of data needed for large area measurements within an acceptable time frame. The intention of this review article is to give an overview of methods used and potentially usable for large area mapping of thin films, with special attention to ellipsometry, the core competence of the authors. The key features include lateral and vertical resolution, speed, sensitivity, but also availability, price and non-destructive capabilities.

In this work, we categorize area (structure) sizes in the context of optical characterization, i.e., compared to the wavelength. (i) In case of structure sizes smaller than the wavelength, usually the effective medium approximation (EMA) holds, considering the materials optically homogeneous, but as a mixture of known reference dielectric functions. (ii) If the characteristic feature sizes are comparable to the wavelength, scattering has to be modeled, which can be used to determine sizes of periodic structures if the period size is in the range of the wavelength. (iii) If the feature sizes are larger than the wavelength, imaging can be applied having a typical resolution determined by the wavelength and the numerical aperture. (iv) The last case is the area size which is much larger than the wavelength (macroscopic, frequently "industrial", meter-sized areas) – in this case both imaging and mapping is applied. Mapping means in our nomenclature that a spot of individual measurements is moved relative to the surface. In this study we mainly focus on case (iv), but partly also consider

This article has been accepted for publication and undergone full peer review but has not been through the copyediting, typesetting, pagination and proofreading process, which may lead to differences between this version and the [Version of Record](#). Please cite this article as [doi: 10.1002/pssa.202100800](https://doi.org/10.1002/pssa.202100800).

case (iii) because many of them have the potential of being scaled up depending on the application.

Methods of thin film and interface characterization can be classified by numerous different aspects such as the way depth profiling is achieved [1], according to illumination and detection [3], or based on in-line capabilities [2]. In section 2 we briefly summarize the many opportunities and in the rest of the paper focus on those potentially applicable to large-area mapping. At the end of this article we discuss some applications and conclude with a short summary of the major characteristics of the methods.

2 Methods of thin film characterization

Abou-Ras and coauthors published a study [1] comparing methods of in-depth thin film characterizations. Three main groups of the approaches have been identified: (i) depth-profiling by sputtering (e.g., secondary ion mass spectrometry [SIMS], secondary neutral mass spectrometry [SNMS], X-ray photoelectron spectrometry [XPS], Auger electron spectrometry [AES], glow-discharge optical emission spectrometry [GD-OES], glow-discharge mass spectrometry [GD-MS], Raman depth profiling), (ii) non-destructive techniques (e.g., spectroscopic ellipsometry [SE], Rutherford backscattering spectrometry [RBS], elastic recoil detection analysis [ERDA], X-ray diffraction [XRD], angle-dependent X-ray emission spectroscopy [AXES]), and (iii) cross-section micro(nano)mapping (e.g., scanning transmission electron microscopy [TEM], its combination with energy dispersive X-ray analysis [EDX], scanning Auger electron microscopy, Raman mapping, time of flight SIMS [TOF-SIMS]). The tools that are capable of the determination of coating thickness are reviewed by Jones et al. [2] sorting the methods in traditional (coulometry, beta particle backscattering, eddy current, magnetic induction, X-ray fluorescence [XRF], X-ray reflectometry [XRR], ultrasonic detection), offline (XPS, scanning electron microscopy [SEM], atomic force microscopy [AFM], GD-OES) and in-line (thermoelectric method, terahertz time domain spectroscopy [THz-TDS], reflectometry, interferometry, ellipsometry, stimulated Brillouin scattering [SBS], self-mixing interferometry [SMI], chromatic confocal microscopy [CCM], infrared thermography) categories with the conclusion of reflectometry, interferometry and ellipsometry being the most suitable methods for in-line characterization.

Sputtering-based depth-profiling and cross-sectional methods require a long measurement time and tedious sample preparation, therefore they are not capable of practical large area mapping. Non-destructive methods such as SE, RBS, ERDA, and AXES require a few minutes or even a few times ten minutes for taking a spectrum at one spot. However, the measurement time of some optical configurations can be reduced to even a few seconds per spot, or a few minutes for a whole mapped or imaged area if using simultaneous measurements at all illuminated lateral positions. We therefore focus primarily on optical methods in this review.

3 Mapping

3.1 Ellipsometry

Ellipsometry determines angle-of-incidence dependent relative amplitude ratios and phase difference shifts of orthogonal electric field components typically defined as parallel and perpendicular to the plane of incidence upon specular reflection of light from a planar surface [4]. Thus, collimated light beams are conventionally used with a well-defined angle of incidence at the reflecting surface. An established method for large-area mapping has been to move both the source and detector units of an ellipsometer in a specular reflection configuration over the surface. This is a widely used standard method for measuring large panels (e.g., solar or display with sizes even over meters) in industrial projects [5,6,7,8]. When measuring in a roll-to-roll (RtR) configuration, the movement of the substrate can also be used as a means of moving the spot on the surface [9]. A

typical application of point-by-point mapping is photovoltaics (PV) because the quality of panels is largely dependent on the lateral uniformity. Ref. [10] shows an example of PV optimization by mapping using the CdS/CdSe/CdTe multilayer structure (Fig. 1). The measurement of one point doesn't take more than a few seconds even using spectroscopy, however, it adds up to hours when measuring thousands of points.

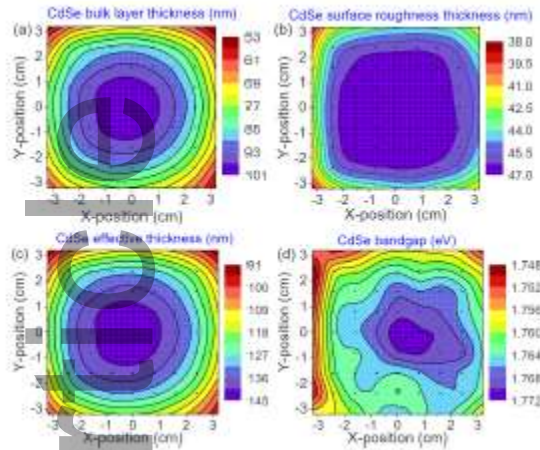


Figure 1: Maps over an area of 65 mm by 65 mm for a CdSe film deposited at room temperature on a high-resistivity transparent layer on a TECTM 15 M substrate including the (a) bulk layer thickness, (b) surface roughness layer thickness, (c) effective thickness and (d) band gap [10].

3.2 Reflection, transmission spectroscopy and scatterometry

A major application of spectroscopic mapping is the characterization of ultrathin 2D materials due to emerging application in optoelectronics and many other areas. An overview of spectroscopic mapping techniques that provide abundant spatial and spectral information can be found in Ref. [11]. Different forms of graphene, molybdenum disulphide (MoS_2), and black phosphorus can be measured by this method. Spatial adsorption and emission, excitonic behavior, light sensitivity, and plasmonic effects, can be investigated and mapped. Hyperspectral line-scanning spectroscopy has been applied for MoS_2 by Dong et al. [12] for thickness mapping and spectral characterization. Hyperspectral imaging microscopy (HSIM) provides abundant spectral information on a surface area rather than a single spot. HSIM has first been applied for microscale imaging of cells and tissues in life sciences [13], food industry [14] and perovskite energy materials [15]. The 3D datacube obtained by HSIM is similar to that measured by divergent light source ellipsometry, but in the latter case the data cube is created in one directional scan of a line on the surface [16, 17], whereas in the usual working modes HSIM includes both line scanning and area scanning options.

A spatially resolved transmission technique was used by Carr et al. [18] for demonstrating a method for large area quality checking in graphene production. A focused beam passes through the sample and is compared with a reference beam obtained by a beam splitter, while the sample is moved by a mapping stage with a spatial resolution of $\approx 10 \text{ } \mu\text{m}$. Using this technique areas over 1 cm^2 can effectively be mapped.

A spatially resolved reflection technique for larger thicknesses (hundreds of microns) is confocal microscopy [19,20] demonstrated by Choi et al. [21] for raster mapping areas as large as 370 mm by 470 mm. Transparent double-layer films have been measured taking into account the numerical aperture of the focusing optics. The non-destructive capability has been emphasized suggesting possible applications for the on-line inspection of multi-layer transparent coatings on flexible substrate during manufacturing. Some optical tomography techniques are also capable of measuring layer thicknesses in tissues in the hundreds of microns thickness range [22].

Scatterometry is applied for mapping surfaces from very small to extremely large [23] scales. Modeling of the diffraction patterns allows to reconstruct complex grating [24] and overlay [25] structures. Point-by-point mapping of an area is also utilized in microscopy by scanning the focused spot while measuring the scattered response – e.g. to measure, find and characterize individual plasmonic nanoparticles by spectroscopy [26].

Imaging scatterometry has been applied for a range of materials from butterfly wings [27, 28] to plasmons [29]. The technique is capable of point-by-point mapping of surfaces, especially because of the imaging technique allows the measurement of the scattered light quickly. However, it has been in most cases only used for one spot [27, 29, 30]. It has been shown that the advanced, phase-detecting version of the method can even be extended to utilize the ellipsometry approach [31].

Single-particle spectra can be measured using an upright optical microscope combined with an aberration corrected imaging spectrometer. Particle size can be well below the applied wavelengths if the average distance between the particles is bigger than the focus size. The sample is mounted on an XYZ piezo stage for precise sample positioning. Illumination and scattered light collection can be performed in epi-illumination using a 100X dark-field objective (Fig. 2).

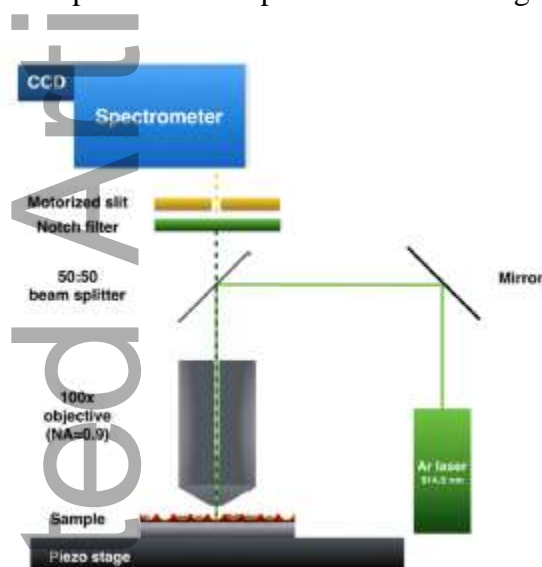


Figure 2: Setup of single-particle mapping spectrometer [30].

The optical measurements can be correlated to scanning electron microscopy (SEM). Accurate sample positioning can be achieved by an XYZ piezo stage mounted on the microscope stage and the actual size and shape of the measured particles can be determined by SEM in nanometer scale. Even complex shaped (only partially covered gold/silica “mushroom”) nanoparticles featuring structural or surface chemical patchiness can be studied [32]. These straightforward methods readily available for gold and silica surface modification using range of different (bio)molecules make these well-defined nanoscale objects excellent candidates to study fundamental processes of programmed self-assembly or application as theranostic agents [33]. Another example is gold nanorods on indium tin oxide substrates which are modified by the combination of nanosphere lithography and ion-bombardment to create a nanopattern with sharp boundaries between the irradiated and masked regions. The single-particle scattering spectra of gold nanorods distributed over the nanopattern can be adequately interpreted in terms of a classical damped harmonic oscillator model, taking the chemical interface damping into account. The damping variations with the related intensity changes can indicate the substrate inhomogeneity at nanometer length scales [34].

3.3 Other methods

A non-destructive tool for the mapping of surface properties is the capillary bridge method. It is related to the measurement of contact angle formed on the solid–liquid–vapor triple line, which has

been one of the most important surface characterization techniques for a long time. The measurement of the advancing and receding contact angles under static conditions on a solid surface enables the quantification of its wettability and the determination of surface free energy, and it provides information about its rough or heterogeneous character. Undoubtedly, the most popular measuring technique is the sessile drop method due to its relative simplicity. Its precision was typically $\pm 2^\circ$ in the past, which was significantly improved ($< \pm 1^\circ$) by the modern axisymmetric drop shape analysis [35]. For low contact angles (typically $< 10^\circ$), the precision of the sessile drop method is not sufficient.

An elegant solution to this problem can be the captive bubble method [36], which inherently fulfills the requirement of saturated vapor. The drawback of this method is that the needle usually must be left in the bubble to hold it in the right place; therefore, the analysis of the bubble's shape is less accurate. The Wilhelmy balance method is another good solution to determine low contact angles. It has high sensitivity and accuracy due to the measurement of wetting force, and it enables to study adsorption processes [37]. There are important requirements to reach this accuracy: the length of the contact line should be known with high precision, i.e., the sample geometry is restricted; furthermore, all surfaces along the contact line must be identical.

To avoid the restrictions of the captive bubble and the Wilhelmy plate techniques, the best method is the contact angle determination on hydrophilic or superhydrophilic surfaces by using $r-\theta$ -type capillary bridges under equilibrium conditions. It enables to determine even ultralow contact angles with high precision without prewetting the investigated surface. In this case, the capillary bridge of the test liquid is formed from a pendant drop and used as a probe. The contact angle is determined from the measured capillary force and liquid bridge geometry by using analytical solution. Contact angles less than 1° can be measured with the uncertainty down to 0.1° [38] This method can be used as a rapid mapping method, too.

Mercury probe Schottky capacitance-voltage (MCV) method is another surface mapping technique for large-area profiling of near-surface carrier density and resistivity in Si epitaxial layers. It is a crucial method in high performance semiconductor manufacturing [39]. MCV systems allow to eliminate the need for costly metal and poly deposition processes by using a pneumatically controlled, non-damaging probe design and a top-side mercury contact. MCV is superior technique both for bulk/epitaxial- and dielectric layer characterization, although the surface preparation technique is crucial for a good measurement [40]. There are a wide range of treatments from wet to dry methods. MCV tool often include electrical characterizations to determine the thickness, k-value and more for dielectrics. Semiconductor-dielectric interface parameters can also be determined from the C-V analysis for compound semiconductors and other special applications.

4 Imaging

4.1 Ellipsometry

Although micro-imaging ellipsometry is a well established technique [41,42,43], much fewer efforts have so far been made for large area imaging of thin films. Our group has proposed a divergent light source configuration for large area imaging. Using this arrangement the surface is illuminated from a divergent point source, and the reflection from the measured surface is imaged by a spherical or parabolic mirror and correction optics to a CCD. All the pixels on the CCD correspond to one point of the sample surface. The modulation of the polarization creates a periodic variation of the intensity in each pixel, from which the map of (Ψ, Δ) pairs can be determined at the given wavelength of illumination. Spectroscopic macro imaging ellipsometry can only be realized in this configuration by measuring maps at different wavelength one-by-one. [16,44]

The 'pin hole-version' of this kind of instrument uses an illumination by an almost diffuse, 'divergent beam' of light that provides a collection of rays with diverse angles of incidence at every

point of the sample. Precise 'angle-selection' is performed on the detector side by a pin-hole camera (Fig. 3). The pin-hole works as an 'angle-of-incidence filter', selecting only one single light-beam from every direction (or sample position). The angular resolution of this type of camera is dependent on the diameter of the pin-hole. In the case of a single wavelength measurement, this instrument is appropriate for measuring a large area sample with possible non-uniform properties such that the pinhole camera selects a single angle of incidence corresponding to each sample point, but that angle varies across the sample. If the sample is moved parallel to its surface and parallel to the plane of incidence along a line during the measurement, however, each sample point will experience multiple angles of incidence successively, which provides additional information to assist in data analysis. This additional information can be useful in the case of anisotropic samples or layers that are inhomogeneous in depth. By repeating the measurement with light of various wavelengths, multi-angle, multi-wavelength (but not continuously spectroscopic) ellipsometry data can be acquired [16,44].

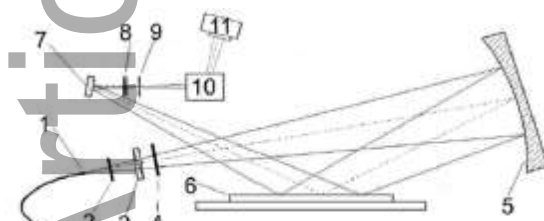


Figure 3: Arrangement of divergent light source ellipsometry. (1) “white” light source, (2) narrow, rectangular aperture, (3) film-polarizer, (4) compensator, (5) spherical mirror, (6) sample, (7) cylindrical mirror, corrected beam, (8) analyzer, (9) pinhole, (10) correction-dispersion optics, (11) CCD detector array.

By confining the number of measured sample points to a narrow range along a line only, we can generate continuous spectroscopic data at each point along the line image using white light illumination with a spectral dispersion (grating) after the pin-hole. This instrument produces spatial information in one dimension of the CCD array simultaneously with spectroscopic information in the perpendicular direction of the array (Fig. 4). Both approaches (multi-angle/multi-wavelength and continuous spectroscopic) are useful, for example, in the analysis of a product moving along a coating line [45, 16, 44, 46, 17] such as in case of a RtR configuration [47].

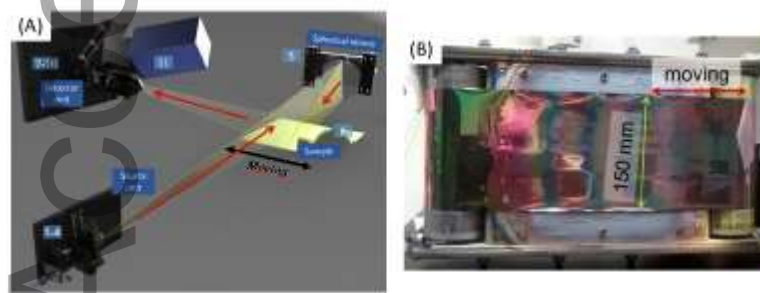


Figure 4: (A) Setup of divergent source spectroscopic mapping ellipsometry using the components of (1) “White” light source, (2) narrow, rectangular aperture, (3) film-polarizer, (4) compensator, (5) spherical mirror (6) sample, (7) cylindrical mirror, corrected beam, (8) analyzer, (9) pinhole, (10) correction-dispersion optics, (11) CCD detector array. (B) Application of divergent source spectroscopic mapping ellipsometry in a RtR configuration. The band is illuminated along a line, whereas the second dimension of the illuminated CCD detector contains the spectroscopic information. By moving the roll, each lateral position of the band is measured spectroscopically. [47]

4.2 Reflectometry

In many cases, complex modeling or nanometer accuracy is not required for the surface mapping. For example, when deviations from an optimal layer structure must be followed, usually a fixed setting for the polarization state and the deviation from this measured by the detected intensity can be followed. It has been shown in several studies that spectroscopic imaging reflectometry [43] is capable of the quantitative measurement of surface layer properties, such as the area fraction of metallic gold layer in Ref. [48] or the layer thickness and roughness of ZnSe films in Ref. [49].

4.3 Scatterometry

Textured surfaces are usually characterized by time-consuming scanning probe or electron microscopy techniques. Imaging scatterometry is a powerful technique to measure extended (larger than a focused spot) areas of structured surfaces with nanometer accuracy [50]. An in-line metrology tool has been demonstrated in Ref. [51] for the dimensional characterization of RtR imprinted nanostructures. It combines real-space imaging with spectral scatterometry. One-dimensional line gratings have been measured using this method. The depth of the structures were accurately characterized with uncertainties of a few nanometers. Light scattering methods have also been applied in medical optics, which includes a wide range of approaches, e.g. fluorescence and inelastic light scattering, coherent effects time-resolved and spatially modulated spectroscopy and tomography, polarization-sensitive techniques, optical coherence tomography and more [52, 53]. In case of low-density plasmonic nanoparticles subwavelength objects can be imaged [30], preferably in dark field configuration [54].

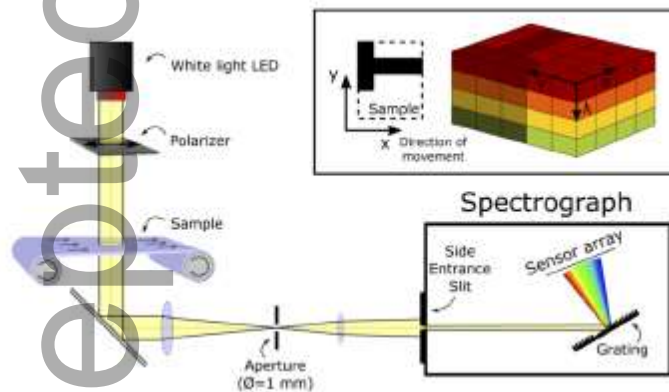


Figure 5: Setup of in-line scatterometer for the dimensional analysis of gratings on a RtR embossing line. The inset shows that the spectroscopic data is continuously collected in the y-direction as the sample is moving to the x-direction. [51]

4.4 Interferometry

Speckle is an interference pattern created by reflection from a non-specular (rough) surface. When a surface is illuminated by laser light, in the reflected image captured by the camera, a granular pattern is obtained. If the particles, certain parts or object on the surface are moving, a time-dependent speckle pattern is generated at each pixel of the camera. The variation of the intensity recorded by each pixel of the camera contains information on the scattered particles. This method has been demonstrated on the two-dimensional mapping of blood flow in the vessels of Sprague-Dawley rats [55]. The method has later been reviewed by Boas and Dunn [52]. There are many ways of improving speckle imaging, including the multi-exposure technique [56].

5 Applications

The capabilities of expanded-beam SE have been demonstrated by numerous prototypes using uncollimated (non-parallel, diffuse) illumination with a detection system consisting of an angle-of-incidence-sensitive pinhole camera for high-speed, large-area imaging/mapping applications. The speed of the measurement system makes the instrument suitable for use on production lines. The precision enables the detection of sub-nm thicknesses, and refractive index and extinction coefficient changes of 0.01. Alternative commercial instruments for SE mapping must translate the sample in two dimensions. Even a sample with a size of 150 mm by 150 mm with a resolution of 10 mm requires >200 measurements and at least 15 minutes. By imaging along one dimension in parallel, the expanded-beam system can measure with similar resolution in 1-2 minutes. The movement in the second dimension can be performed in robotic arm (Fig. 6) or RtR [47] (Fig. 7) configurations. It has been demonstrated that 300-mm diameter Si wafers covered by amorphous NiSi (a-NiSi) and ion-implanted using plasma immersion can be measured on a robotic arm in a clean room environment (Fig. 6). The agreement of the determined layer thickness compared to the point-by-point measurement of a commercial Semilab-SOPRA ellipsometry is good (within one nm), while the duration of the measurement is at least an order of magnitude shorter on a divergent light source mapping ellipsometer. NiSi layers on a 300 mm diameter Si wafer are interesting in microelectronic fabrication where the silicide layers with controlled thickness can be used as ohmic- or Schottky-contacts. The homogeneity is important if we consider that the fabricated chip-parameters should be within the fabrication tolerance limits of the chip.

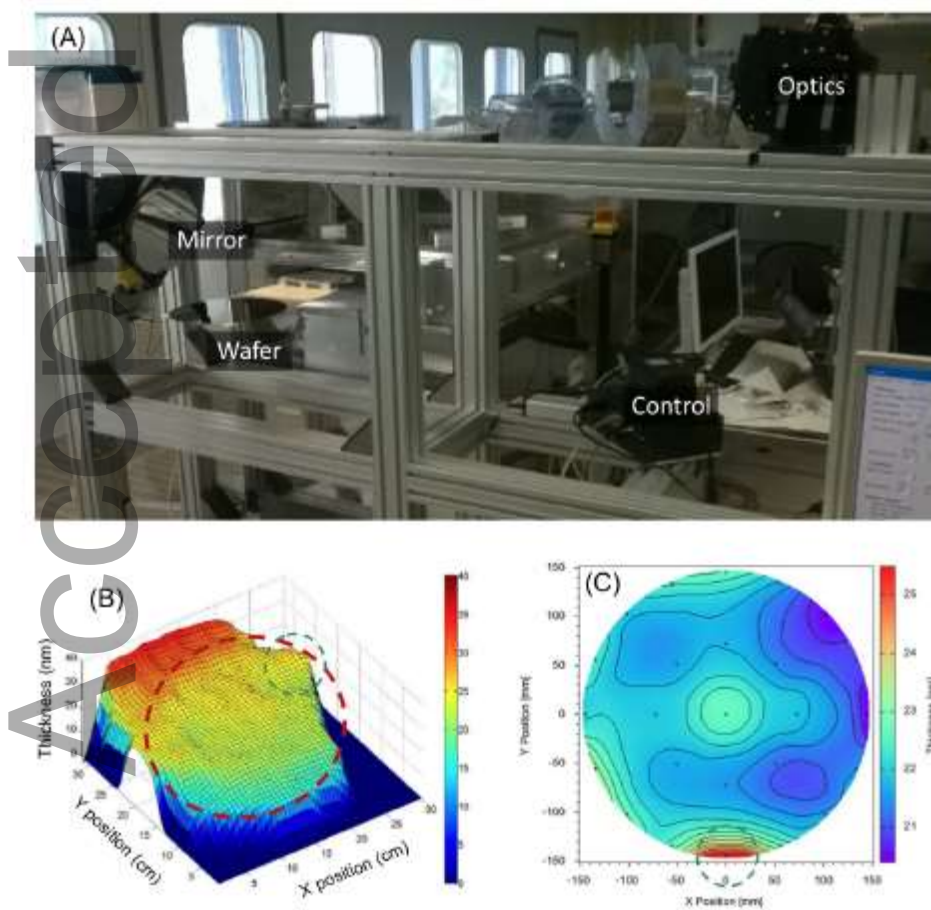


Figure 6: (A) Prototype of a macro-imaging spectroscopic ellipsometer for the measurement on a robotic arm of a cluster tool for 300-mm wafers. The mirror for the imaging is in the top left corner of the metal frame, next to the wafer on the robotic arm. All other optical components are located in the unit in the top right corner of the image. (B) Thickness map of a-NiSi on a 300-mm diameter wafer

measured by divergent beam mapping ellipsometry during the movement of the robotic arm of the cluster tool. (C) Reference measurement on the sample of figure (B) by a commercial Semilab-SOPRA ellipsometer using the point-by-point method.

Expanded-beam SE was applied for the imaging/mapping analysis of large area spatial uniformity of multilayer-coated substrates in RtR thin film PV [47]. The instrument allows width-wise imaging and length-wise mapping for uniformity evaluation at the high linear substrate speeds required for real-time, in-situ, and on-line analysis in RtR thin film PV: Ag, ZnO, and n-type hydrogenated amorphous Si (a-Si:H) layers of an a-Si:H n-i-p structure deposited on a flexible polyimide substrate in the RtR configuration. SE data across a line image were collected as the substrate was translated by a RtR mechanism. A coated area of 450 mm by 120 mm was analyzed for layer thickness and optical properties by applying the appropriate analytical models for the complex dielectric functions of the Ag, ZnO and n-type Si:H layers. In the case of the a-Si/ZnO/Ag/plastic-foil structure, we measured first the ZnO-layer only on the {Ag layer}/{plastic foil} RtR sample and moved the cassette RtR model machine into the a-Si deposition chamber. After the a-Si deposition the cassette RtR model machine was moved back to the measurement chamber (without breaking the vacuum) and measured again by the expanded beam mapping SE (see Fig. 7).

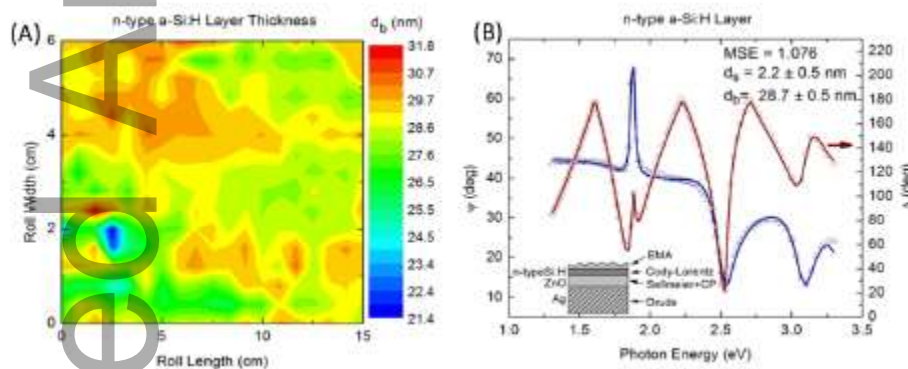


Figure 7: (A) Map of thickness of the a-Si layer on top of a ZnO layer on Ag in a structure used for PV. The measurement has been made in a RtR configuration. (B) Measured (symbols) and fitted (lines) ellipsometry spectra used for the calculation of the sample properties, the thickness of which is shown in (A). The inset shows the optical model in which the dispersions of the a-Si and ZnO layers were described using the Cody-Lorentz [57] and the Sellmeier+critical point models [58], respectively.

Optical model of similar complexity was demonstrated for a ZnO/Mo/glass structure. This structure is also used in the photovoltaics where the ZnO layer can be used as a transparent conductive layer which also serves as an optimized back-reflector. The investigated sample was a glass plate covered by Mo and a ZnO layer (Fig. 8A). The investigated area was 300 mm by 300 mm (Fig. 8B), demonstrating the compatibility with the current 300-mm wafer technology of the semiconductor industry. A reference measurement was performed on the same sample using a Woollam M-2000DI ellipsometer (Fig. 8C). Using this instrument, the maximum area for mapping is 150 mm by 150 mm (Fig. 8D). The thickness determined by the expanded-beam instrument agrees within a few nanometer, however, the duration of the measurement for the same resolution is an order of magnitude smaller.

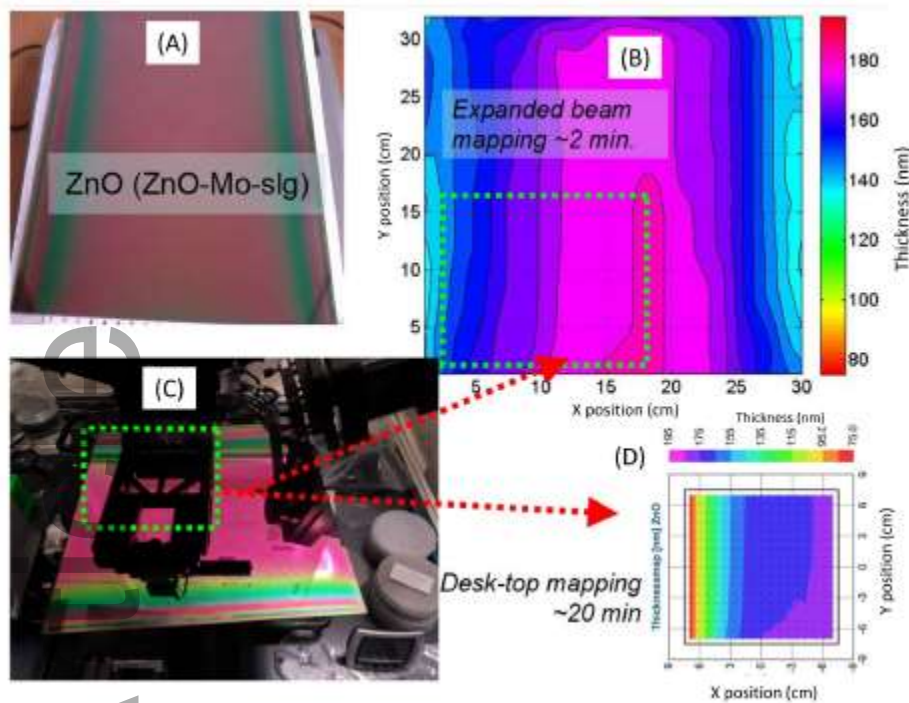


Figure 8: (A) Glass plate (width of approximately 300 mm) covered by Mo and ZnO. (B) An area compatible with the 300-mm technology of the semiconductor industry was investigated by the expanded-beam ellipsometer. The duration of the data acquisition was ≈ 2 minutes. The thickness is color-coded in steps of 10 nm. (C) Glass plate on the mapping stage of a Woollam M-2000DI ellipsometer. (D) Mapping measurement by the M-2000DI ellipsometer in a rectangular area of 150 mm by 150 mm.

The compatibility of divergent-source mapping ellipsometry with the 450-mm wafer technology was demonstrated by measuring an area covered by individual thermally oxidized 4-inch wafers. The thicknesses of the SiO_2 layers were different in different rows showing that even highly inhomogeneous large-area samples can be mapped easily. Fig. 9A shows an overview of the fit quality (MSE) on the whole surface, demonstrating that the optical model of Fig. 9 is valid for the regions covered by the 4-inch wafers. Fig. 9 zooms into specific areas by plotting the thickness of the SiO_2 layer determined from the model. Note that a good agreement was obtained between the measured and the fitted curves by only using two fit parameters (Fig. 9E), the thickness and the non-uniformity.

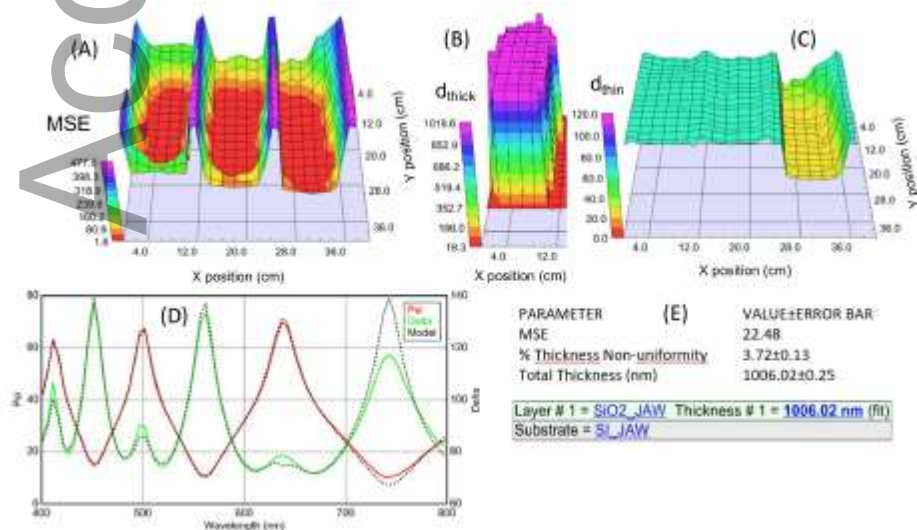


Figure 9: Large area mapping assembled from 9 different oxidized 4-inch Si wafers. (A) Mean square error (MSE) map describing the quality of the fit over the whole surface. (B) and (C) are maps of nominally 1000 and 25-60 nm thick samples with a magnified (max. 120 nm, 1 color = 10 nm) scale. (D) Measured and fitted spectra from the 1000-nm area. (E) Model parameters and uncertainties used for the fit.

The size of the illuminated area of the expanded beam ellipsometer [17] can be adjusted for the task. Fig. 10 shows an extreme case in which the area of mapping was 1000 mm by 500 mm on a glass panel used for solar applications. The glass is covered by a-Si. Each map represents a set of ellipsometric spectra that are analyzed and fitted by an optical model. In Fig. 10 maps of the parameters of thickness (Fig. 10A) and band gap (Fig. 10B) are plotted. The accuracy of the measurement has been verified using a Woollam M2000 ellipsometer, and the agreement was within a few percent, similar to other cases comparing the expanded beam ellipsometer with reference measurements on commercial tools.

The thin film PV technology is more cost-effective than using bulk material (the same w_{peak} costs less because less energy is needed to prepare the thin films than the bulk crystalline-silicon, therefore, the energy pay-back time is also better), but it requires a good lateral homogeneity. Commercial instruments using 1D detector arrays for SE must translate either the sample or the ellipsometer in two dimensions in order to map large area samples. A sample size of 150 mm by 150 mm requires more than 200 measurements and at least 15 minutes of measurement time to achieve a spatial resolution of 10 mm. By using a 2D detector array and imaging along one dimension in parallel, the sample needs only be translated in one dimension in order to map large area samples. As a result, the expanded-beam system that provides a line image of SE (wavelength from 350 to 1000 nm) can measure with similar spatial resolution in less than 2 minutes. Incorporating the results of real time SE measurements, which provide proper initial parameters in least-squares regression for the analysis of the imaging/mapping data, expanded beam ellipsometry can be an effective in-line monitor of uniformity in PV production lines using RtR or rigid plate substrates. The goal of near future efforts is to increase the speed by 4. Then 1800 points could be mapped in a 1 minute traverse of a PV panel over an area as large as 1000 mm by 500 mm using a continuous measurement with a simultaneous evaluation.

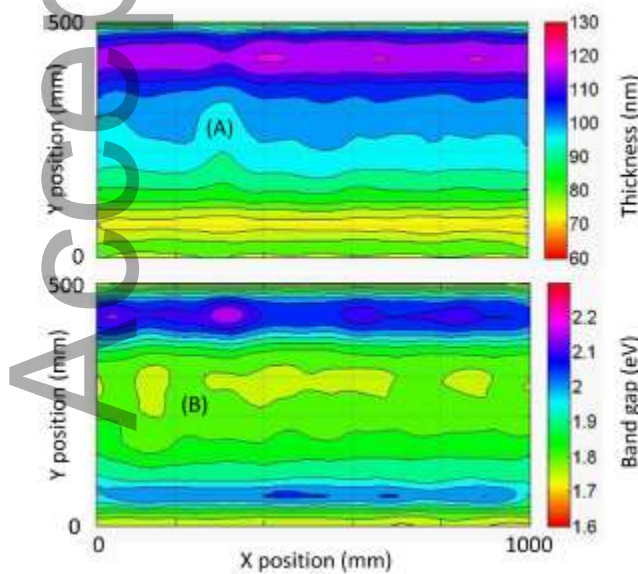


Figure 10: Thickness (A) and band gap (B) maps of a-Si layer on a glass panel.

6 Conclusions

Methods of large-area thin film characterization have been summarized. According to other studies [2] only optical methods are capable of a high-speed, high-sensitivity and non-destructive characterization of thin films over large surfaces (although some potential future candidates have also been mentioned, such as the thermoelectric method with a magnetic readout approach, terahertz time-domain spectroscopy, chromatic confocal microscopy, infrared thermography, as well as XRR or XRF). In case of optical methods we discussed techniques including spectroscopic reflectometry, transmission, scattering, speckle imaging and SE in all cases when the areas under study were larger than the wavelength of light. Only two methods have been identified that are capable of mapping or imaging meter-sized areas (Table 0). One of them moves an ellipsometry head over the surface utilizing point-by-point mapping [10]. Divergent light source macro imaging SE [17,47] is, however, capable of increasing the speed of large area measurement by at least an order of magnitude utilizing imaging, measuring multiple points over the surface simultaneously by SE, maintaining the capabilities of complex modeling and nanometer-scale sensitivity. In the applications section a broad range of examples have been demonstrated about the capabilities of this method.

Table 1: Features of selected optical methods suitable for surface mapping. Area and Speed stand for an approximation of the best values, i.e. the largest area and the smallest time for mapping the area. Please note that the values given here are rough estimations, which may significantly differ from instrument to instrument, from sample to sample (e.g. reflectivity) and from other requirements (noise reduction, accuracy, spectral range, etc.).

Method	Area	Time
Macro imaging SE	Meter(s)	Seconds for one wavelength, minutes for spectroscopy ($\approx 10^3$ points)
Imaging SE	Millimeters	Seconds for one wavelength, minutes for spectroscopy ($\approx 10^6$ points)
Imaging spectroscopy, scatterometry or interferometry (speckle)	Meter(s) (but demonstrations only for much smaller sizes)	Seconds to minutes
Mapping SE	Meter(s)	Seconds for one point, hours for $\approx 10^3$ points (spectroscopy)
Mapping spectroscopy or scatterometry	Meter(s) (but demonstrations only for much smaller sizes)	Minutes or hours

acknowledgements

Support from the National Development Agency Grants of OTKA Nr. K313515 and K129009 are greatly acknowledged.

conflict of interest

The authors declare that they have no known competing financial interests or personal relationships that could have appeared to influence the work reported in this paper.

References

- [1] Abou-Ras D, Caballero R, Fischer CH, Kaufmann CA, Lauermann I, Mainz R, et al. Comprehensive Comparison of Various Techniques for the Analysis of Elemental Distributions in Thin Films. *Microscopy and Microanalysis* 2011;17:728–751.
- [2] Jones A, Uggalla L, Li K, Fan Y, Willow A, Mills CA, et al. Continuous In-Line Chromium Coating Thickness Measurement Methodologies: An Investigation of Current and Potential Technology. *Sensors* 2021;21:3340.
- [3] Kalas B, Agocs E, Romanenko A, Petrik P. In Situ Characterization of Biomaterials at Solid-Liquid Interfaces Using Ellipsometry in the UV-Visible-NIR Wavelength Range. *physica status solidi (a)* 2019;216:1800762.
- [4] Fujiwara H. *Spectroscopic Ellipsometry: Principles and Applications*. Spectroscopic Ellipsometry: Principles and Applications; 2007. Pages: 369.
- [5] SEMILAB, Imaging Spectroscopic Reflectometry;. <https://semilab.com/category/products/imaging-spectroscopicreflectometry->
- .
- [6] SEMILAB, Spectroscopic Ellipsometry;. <https://semilab.com/category/products/spectroscopic-ellipsometry-..>
- [7] Woollam, Theta-SE ellipsometer;. <https://www.jawoollam.com/products/theta-se-ellipsometer>.
- [8] Osborne M. New Product: J.A. Woollam's AccuMap-SE provides thin film measurement of panel uniformity. *PCTech* 2010 Feb; https://www.pv-tech.org/new_product_j-a_woollams_accumap-se_provides_thin_film_measurement_of_panel/.
- [9] Logothetidis S, Georgiou D, Laskarakis A, Koidis C, Kalfagiannis N. In-line spectroscopic ellipsometry for the monitoring of the optical properties and quality of roll-to-roll printed nanolayers for organic photovoltaics. *Solar Energy Materials and Solar Cells* 2013;112:144–156.
- [10] Razooqi Alaani MA, Koirala P, Pradhan P, Phillips AB, Podraza NJ, Heben MJ, et al. Tailoring the CdS/CdSe/CdTe multilayer structure for optimization of photovoltaic device performance guided by mapping spectroscopic ellipsometry. *Solar Energy Materials and Solar Cells* 2021;221:110907.
- [11] Dong X, Yetisen AK, Köhler MH, Dong J, Wang S, Jakobi M, et al. Microscale Spectroscopic Mapping of 2D Optical Materials. *Advanced Optical Materials* 2019;7:1900324.
- [12] Dong X, Dong J, Yetisen AK, Köhler MH, Wang S, Jakobi M, et al. Characterization and layer thickness mapping of two-dimensional MoS₂ flakes via hyperspectral line-scanning microscopy. *Applied Physics Express* 2019;12:102004.
- [13] Cucci C, Delaney JK, Picollo M. Reflectance Hyperspectral Imaging for Investigation of Works of Art: Old Master Paintings and Illuminated Manuscripts. *Accounts of Chemical Research* 2016;49:2070–2079.
- [14] Liu Y, Chen YR, Kim MS, Chan DE, Lefcourt AM. Development of simple algorithms for the detection of fecal contaminants on apples from visible/near infrared hyperspectral reflectance imaging. *Journal of Food Engineering* 2007;81:412–418.

- [15] Alexander-Webber JA, Faugeras C, Kossacki P, Potemski M, Wang X, Kim HD, et al. Hyperspectral Imaging of Exciton Photoluminescence in Individual Carbon Nanotubes Controlled by High Magnetic Fields. *Nano Letters* 2014;14:5194–5200.
- [16] Juhász G, Horváth Z, Major C, Petrik P, Polgár O, Fried M. Non-collimated beam ellipsometry. *physica status solidi (c)* 2008;5:1081–1084.
- [17] Fried M, Juhász G, Major C, Petrik P, Polgár O, Horváth Z, et al. Expanded beam (macro-imaging) ellipsometry. *Thin Solid Films* 2011;519:2730–2736.
- [18] Carr AJ, DeGennaro D, Andrade J, Barrett A, Bhatia SR, Eisaman MD. Mapping graphene layer number at few-microns scale spatial resolution over large areas using laser scanning. *2D Materials* 2020;8:025001.
- [19] Török P, Varga P, Laczik Z, Booker GR. Electromagnetic diffraction of light focused through a planar interface between materials of mismatched refractive indices: an integral representation. *JOSA A* 1995;12:325–332.
- [20] Török P, Hewlett SJ, Varga P. The role of specimen-induced spherical aberration in confocal microscopy. *Journal of Microscopy* 1997;188:158–172.
- [21] Choi YM, Yoo H, Kang D. Large-area thickness measurement of transparent multi-layer films based on laser confocal reflection sensor. *Measurement* 2020;153:107390.
- [22] Mujat M, Chan RC, Cense B, Park BH, Joo C, Akkin T, et al. Retinal nerve fiber layer thickness map determined from optical coherence tomography images. *Optics Express* 2005;13:9480–9491.
- [23] Long DG, Hardin PJ, Whiting PT. Resolution enhancement of spaceborne scatterometer data. *IEEE Transactions on Geoscience and Remote Sensing* 1993;31:700–715.
- [24] Kumar N, Petrik P, Ramanandan GKP, El Gawhary O, Roy S, Pereira SF, et al. Reconstruction of sub-wavelength features and nano-positioning of gratings using coherent Fourier scatterometry. *Optics Express* 2014;22:24678.
- [25] Huang HT, Raghavendra G, Sezginer A, Johnson K, Stanke FE, Zimmerman ML, et al. Scatterometry-based overlay metrology. vol. 5038; 2003. p. 126–137.
- [26] Szekrényes DP, Pothorszky S, Zámbo D, Deák A. Detecting spatial rearrangement of individual gold nanoparticle heterodimers. *Physical Chemistry Chemical Physics* 2019;21:10146–10151.
- [27] Stavenga DG, Leertouwer HL, Pirih P, Wehling MF. Imaging scatterometry of butterfly wing scales. *Optics Express* 2009;17:193–202.
- [28] Wilts BD, Leertouwer HL, Stavenga DG. Imaging scatterometry and microspectrophotometry of lycaenid butterfly wing scales with perforated multilayers. *Journal of The Royal Society Interface* 2009;6.
- [29] Constant TJ, Hibbins AP, Lethbridge AJ, Roy Sambles J, Stone EK, Vukusic P. Direct mapping of surface plasmon dispersion using imaging scatterometry. *Applied Physics Letters* 2013;102:251107.
- [30] Zámbo D, Szekrényes DP, Pothorszky S, Nagy N, Deák A. SERS Activity of Reporter-Particle-Loaded Single Plasmonic Nanovoids. *The Journal of Physical Chemistry C* 2018;122:23683–23690.
- [31] Petrik P, Kumar N, Fried M, Fodor B, Juhász G, Pereira SF, et al. Fourier ellipsometry – an

ellipsometric approach to

Fourier scatterometry. *Journal of the European Optical Society: Rapid Publications* 2015;10:15002.

[32] Pothorszky S, Zámbo D, Deák A. Structural and Optical Properties of Gold/Silica “Mushroom” Particles Prepared by

Interfacial Templating. *Particle & Particle Systems Characterization* 2017;34:1600291.

[33] Szekrényes DP, Kovács D, Zolnai Z, Deák A. Chemical Interface Damping as an Indicator for Hexadecyltrimethylammonium

Bromide Replacement by Short-Chain Thiols on Gold Nanorods. *The Journal of Physical Chemistry C*

2020;124:19736–19742.

[34] Zolnai Z, Zámbo D, Osváth Z, Nagy N, Fried M, Németh A, et al. Gold Nanorod Plasmon Resonance Damping Effects on

a Nanopatterned Substrate. *The Journal of Physical Chemistry C* 2018;122:24941–24948.

[35] Rotenberg Y, Boruvka L, Neumann AW. Determination of surface tension and contact angle from the shapes of axisymmetric

liquid interfaces. *Journal of Colloid and Interface Science* 1983;93:169–183.

[36] Taggart AF, Taylor TC, Ince CR. Experiments with flotation reagents. American Institute of Mining and Metallurgical

Engineers, Incorporated; 1929.

[37] Volpe CD, Siboni S. The Wilhelmy method: a critical and practical review. *Surface Innovations* 2018;6:120–132.

[38] Nagy N. Contact Angle Determination on Hydrophilic and Superhydrophilic Surfaces by Using r-Type Capillary Bridges.

Langmuir 2019;35(15):5202–5212.

[39] Zhang W, Song C, Xue K, Yang S, Yong Z, Li H, et al. Silicon interposer process development for advanced system

integration. *Microelectronic Engineering* 2016;156:50–54.

[40] Sanna C, Taylor P, Hillard R, Frey S, McDonald D, Hoglund J, et al. Assessment of Surface Preparation Methods for

Mercury (Hg) Probe Schottky Capacitance-Voltage (MCV) on Epitaxial Silicon. *ECS Journal of Solid State Science and*

Technology 2021;10:074006.

[41] Wurstbauer U, Röling C, Wurstbauer U, Wegscheider W, Vaupel M, Thiesen PH, et al. Imaging ellipsometry of graphene.

Applied Physics Letters 2010;97:231901.

[42] Rosu D, Petrik P, Rattmann G, Schellenberger M, Beck U, Hertwig A. Optical characterization of patterned thin films.

Thin Solid Films 2014;571:601–604.

[43] Necas D, Ohlídal I, Franta D, Cudek V, Ohlídal M, Vodák J, et al. Assessment of non-uniform thin films using spectroscopic

ellipsometry and imaging spectroscopic reflectometry. *Thin Solid Films* 2014;571:573–578.

[44] Major C, Juhász G, Horváth Z, Polgar O, Fried M. Wide angle beam ellipsometry for extremely large samples. *physica*

status solidi (c) 2008;5:1077–1080.

[45] Horváth ZG, Juhász G, Fried M, Major C, Petrik P, Imaging optical inspection device with a pinhole camera. Patent; 2008.

<https://patentscope.wipo.int/search/en/detail.jsf?docId=WO.>, patent Number:

PCT/HU2008/000058.

[46] Major C, Juhász G, Petrik P, Horváth Z, Polgár O, Fried M. Application of wide angle beam spectroscopic ellipsometry

for quality control in solar cell production. *Vacuum* 2009;84:119–122.

[47] Shan A, Fried M, Juhász G, Major C, Polgar O, Nemeth A, et al. High-Speed Imaging/Mapping

This article is protected by copyright. All rights reserved

Spectroscopic Ellipsometry

for In-Line Analysis of Roll-to-Roll Thin-Film Photovoltaics. *IEEE Journal of Photovoltaics* 2014;4:355–361.

[48] Vodák J, Necas D, Pavlinák D, Macak JM, Ricica T, Jambor R, et al. Application of imaging spectroscopic reflectometry for characterization of gold reduction from organometallic compound by means of plasma jet technology. *Applied Surface Science* 2017;396:284–290.

[49] Necas D, Ohlídal I, Franta D, Ohlídal M, Vodák J. Simultaneous determination of optical constants, local thickness and roughness of ZnSe thin films by imaging spectroscopic reflectometry. *Journal of Optics* 2015;18:015401.

[50] Madsen MH, Hansen PE. Imaging scatterometry for precise measurements of patterned areas. *Optics Express* 2016;24:1109–1117.

[51] Skovlund Madsen J, Geisler M, Berri Lotz M, Zalkovskij M, Bilenberg B, Korhonen R, et al. In-line characterization of nanostructures produced by roll-to-roll nanoimprinting. *Optics Express* 2021;29:3882.

[52] Boas DA, Dunn AK. Laser speckle contrast imaging in biomedical optics. *Journal of Biomedical Optics* 2010;15:011109.

[53] Tuchin VV. *Tissue Optics: Light Scattering Methods and Instruments for Medical Diagnosis*. Society of Photo-Optical Instrumentation Engineers (SPIE); 2015.

<http://ebooks.spiedigitallibrary.org/book.aspx?doi=.•...../...•••••>

[54] Xie YF, Liu ML, Lv WY, Li X, Gao PF, Li YF, et al. Metal-Mediated Gold Nanospheres Assembled for Dark-Field Microscopy Imaging Scatterometry. *Talanta* 2019;201:280–285.

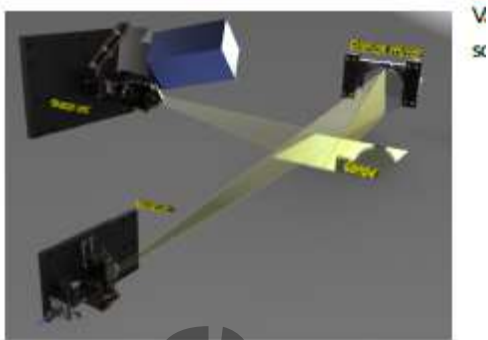
[55] Cheng H, Luo Q, Zeng S, Chen S, Cen J, Gong H. Modified laser speckle imaging method with improved spatial resolution. *Journal of Biomedical Optics* 2003;8:559.

[56] Parthasarathy AB, Tom WJ, Gopal A, Zhang X, Dunn AK. Robust flow measurement with multi-exposure speckle imaging. *Optics Express* 2008;16:1975–1989.

[57] Ferlauto AS, Ferreira GM, Pearce JM, Wronski CR, Collins RW, Deng X, et al. Analytical model for the optical functions of amorphous semiconductors from the near-infrared to ultraviolet: Applications in thin film photovoltaics. *Journal of Applied Physics* 2002;92:2424–2436.

[58] Petrik P. Parameterization of the dielectric function of semiconductor nanocrystals. *Physica B: Condensed Matter* 2014;453:2–7.

GRAPHICAL ABSTRACT



Vacuum integrable in-situ ellipsometry as an example of spectroscopic macro-imaging optical measurement on a RtR substrate



Peter Petrik received his M.Sc and Ph.D degrees from the Technical University of Budapest in engineering and physics, respectively. He was a visiting scientist in Germany, USA, and the Netherlands for a total of more than 5 years. He is dealing with materials science and the development of ellipsometry. He was the first winner of the Drude Award founded at the 4th International Conference on Spectroscopic Ellipsometry in 2007 for "exceptional contributions to the development and application of spectroscopic ellipsometry". He is the head of the Photonics department of the Centre for Energy Research of the Loránd Eötvös Research Network.



Miklos Fried received his M.Sc and Ph.D degrees from the Roland Eötvös University in 1982 and 1985, respectively. He was a visiting scientist in the MESA Research Institute (University of Twente, Enschede, The Netherlands, 1995-98) and at the Lehrstuhl für Elektronische Bauelemente der Friedrich-Alexander Universität Erlangen-Nürnberg, Germany (1997-99). He was the Hungarian project-leader of the RESPECT-COPERNICUS (REal-time evaluation of SPECTroscopic data)

multilateral (Dutch, Hungarian, Czech), the Semiconductor Equipment Assessment for Key Enabling Technologies (SEA4KET) and European 450mm Equipment Demo Line (E450EDL) EU-cooperations. His main research field is the investigation of surface modification of materials by ellipsometry and ion backscattering spectrometry.

Accepted Article